

ANALYSIS OF MOVING BOUNDARY PROBLEM OF GROWTH OF BISMUTH GERMANATE CRYSTAL BY HEAT EXCHANGER METHOD

Jong Hoe Wang, Do Hyun Kim[†] and Dae-Shik Chung*

Dept. of Chem. Eng./Proc. Anal. Lab., KAIST, Taejon 305-701, Korea

*Ceramics Team, RIST, Pohang 790-600, Korea

(Received 10 May 1996 • accepted 26 August 1996)

Abstract - Transient two-dimensional model of the growth of BGO crystal by heat exchanger method has been developed. A finite element method with nonorthogonal mapping technique for the solution of the moving boundary problem is developed where the melt/solid interface shape changes from hemispherical to planar. The moving boundary problems for the melt/solid interface location and the temperature field were solved by two mapping rule method which enables the computation of interface shape changing from hemispherical to planar. The maximum deflection of interface is shown when the melt/solid interface meets the corner of crucible. As the excess heating temperature and the heat exchanger temperature were increased, more growth time for whole process is required but the quality of BGO crystal may be improved. The ratio of the height to the radius of crucible hardly affects the deflection of BGO melt/solid interface when it is greater than 1.5. As the cooling zone radius is decreased, maximum deflection is decreased. The heat transfer between the crucible and the heating element should be suppressed to maximize planarity of the interface shape.

Key words: Heat Exchanger Method, Bismuth Germanate, Finite Element Method, Moving Boundary Problem, Non-orthogonal Mapping

INTRODUCTION

Since Weber and Monchamp [1973] measured the luminescence spectra and decay properties of bismuth germanate ($\text{Bi}_2\text{Ge}_2\text{O}_{12}$) and predicted it to be a new scintillator material, the research on growth, performance and application of BGO has been developed successfully. Bridgman [Fan et al., 1991; Kawano et al., 1993], Czochralski [Takagi and Fukazawa, 1986; Berkowski et al., 1991] and float-zone [Quon et al., 1993] techniques have been employed to grow BGO single crystals which have great potential for technological application in solid-state devices.

The Heat Exchanger Method (HEM) is a process which controls both the heat input and the heat extraction independently in a crystal growth furnace. The HEM furnace has a well-insulated heating element in which there are no intrinsic temperature gradient. At the base of the crucible, the heat exchanger provides the control of heat extraction, allowing precise control of the temperature gradients necessary for crystal growth. The schematic diagram of a HEM furnace is shown in Fig. 1(a).

In the HEM, the melt is nearly kept at constant temperature while growth of the crystal is controlled by the thermal gradient within the solid provided by the helium flow in the heat exchanger. The melt/solid interface at the beginning of the solidification takes a hemispherical shape and the temperature of melt/solid interface is constant at any given point. Since the distance between the crucible and the melt/solid interface is changed as the growth continues, the temperature gradient in the melt is varied [Kaldis, 1985]. This leads to the convex melt/solid interface. A flat melt/solid interface can be achieved by controlling both the heat input and extraction.

Many numerical methods have been used to solve the steady-state free-and transient moving-boundary problems [Lynch and Gray, 1980; Gelinis, 1981; Saito and Scriven, 1981; Ettouney and Brown, 1983; Gallagher et al., 1984; Ungar et al., 1988]. Ettouney and Brown [1983] classified the numerical methods for solving free-boundary problems and presented especially the Isotherm-Newton algorithm. Several finite element techniques have been proposed for moving elements and these are reviewed by Lynch and Gray [1980]. Ungar et al. [1988] built the time-integration methods for solution of the transient moving-boundary problem that describes microstructure formation based on the finite-element-Newton algorithm by Ettouney and Brown [1983] for solution of steady-state free-boundary problem. Although many free- and moving-boundary problems have been solved by using the original coordinate system with the moving meshes or transforming the problem to a fixed domain, the transition of the interface shape from hemispherical to planar cannot be simulated by these methods.

In this paper, the model for heat transfer in the HEM for growth of BGO crystal was developed. This model includes melt/solid BGO, heat exchanger and heating element. A reliable numerical method for transient simulation of the transition of melt/crystal interface shape has been developed and a nonorthogonal mapping technique designed for computing it is introduced. With the mathematical model and the numerical method, the effects of the various growth parameters were examined on the interface shape and the temperature field.

MATHEMATICAL MODEL

The HEM model for the growth of BGO crystal has been developed to simulate the heat transfer process. The solutions

[†]To whom all correspondences should be addressed.

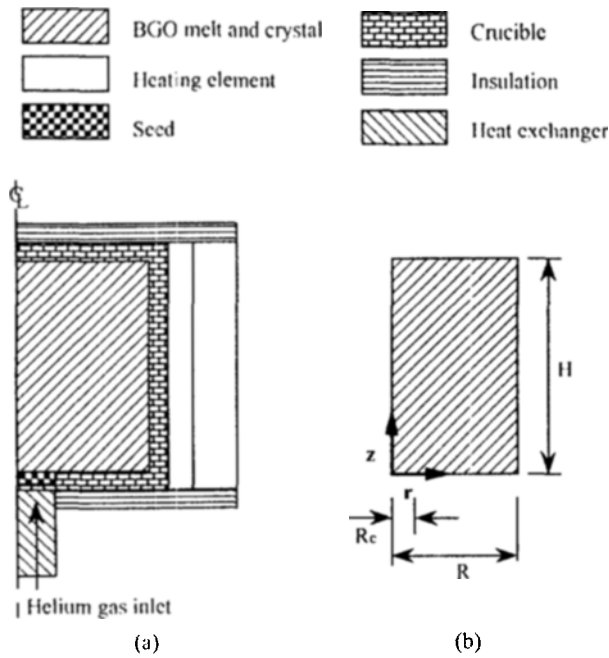


Fig. 1. A typical HEM furnace and the numerical domain of the model.

from the model include the location of the melt/solid interface and temperature field in the crucible. The interface location of melt/solid is determined simultaneously by the equilibrium (isotherm) condition along the interface [Ettouney and Brown, 1983].

The thermophysical properties of the solid and liquid BGO are assumed to be same and the latent heat effect is neglected. The hottest liquid is on the top and coolest on the bottom during the crystal growth by HEM. This minimizes convection in the melt due to the stabilizing temperature gradient [Schmid et al., 1994]. Prandtl number of BGO is about 0.1 [Kawano et al., 1993; Shigematsu et al., 1994] that the convective heat transfer in the melt is neglected.

The geometry of the mathematical model for HEM growth of BGO crystal is shown in Fig. 1(b). The computational domain is crucible which contains the melt and solid BGO.

The energy equation [Bird et al., 1960] is

$$\frac{\partial T}{\partial t} = \alpha \left[\frac{1}{r} \frac{\partial}{\partial r} \left(r \frac{\partial T}{\partial r} \right) + \frac{\partial^2 T}{\partial z^2} \right] \quad (1)$$

where α is the thermal diffusivity of BGO. The interface location of melt/solid BGO is obtained by the equilibrium condition along the interface

$$T = T_m \quad (2)$$

where T_m is the melting temperature of BGO.

The solutions of the transient second-order partial differential equation require the initial condition and boundary conditions. The initial condition is

$$T(r, z, 0) = T_m + \Delta T \quad (3)$$

where ΔT is the excess heating temperature which is defined as the difference between the initial melt temperature and the melt-

Table 1. The growth parameters

Growth parameters	Meaning	Values
T_m	Melting temperature of BGO	1050°C
α	Thermal diffusivity of BGO	0.3077 cm ² /sec
R	Crucible radius	1.5 cm
ΔT	Excess heating temperature of melt	25-150°C
R_c	Cooling zone radius	0.15-0.375 cm
H	Crucible height	1.5-4.5 cm
Bi	Dimensional Biot number	0-10 ⁻¹ cm ⁻¹
T_o	Heat exchanger temperature	250-750°C

ing temperature of BGO.

The boundary conditions are

$$\frac{\partial T(0, z, t)}{\partial r} = 0 \quad (4)$$

$$\frac{\partial T(R, z, t)}{\partial r} = Bi(T_\infty - T) \quad (5)$$

$$T(r, 0, t) = T_o, \quad 0 \leq r \leq R_c \quad (6)$$

$$\frac{\partial T(r, 0, t)}{\partial z} = 0, \quad R_c \leq r \leq R \quad (7)$$

$$\frac{\partial T(r, H, t)}{\partial z} = 0 \quad (8)$$

where the *dimensional* Biot number Bi is used for considering the conductive and convective heat transfer between the crucible and the heating element. Bi has the dimension of [cm⁻¹]. T_∞ is the temperature of heating element and the initial melt temperature is ($T_m + \Delta T$). T_o is the temperature of heat exchanger. The growth parameters used for calculations are summarized in Table 1.

Eqs. (1)-(8) define a moving-boundary problem for the temperature fields in melt and crystal and the shape of melt/crystal interface. The solutions of the equation set can be obtained easily when the melt and solid BGO are assumed to be in the single phase. Solutions for the single phase case is used as a base for comparison with two phase solution having melt/solid interface. In this paper, the interface locations are computed simultaneously as a part of solution.

NUMERICAL METHOD

The moving boundary problem for the melt/crystal interface shape and the temperature field is solved using finite element Isotherm-Newton method. The problem is mapped to a fixed domain using the transformations shown in Table 2. Transient HEM model is reduced to the residual equations by applying the Galerkin finite element method. The Newton iteration scheme was used for solving the nonlinear algebraic equation set and the implicit Euler algorithm was used for the time integration [Finlayson, 1980]. The resulting set of linear equations were solved using frontal solver developed by Hood [1976].

1. Transformation Rules

The moving boundary problem of Eqs. (1)-(8) is mapped to the coordinate system (ξ, η) to explicitly express the non-

Table 2. The mapping rules used in finite element formulations

Mapping I			
Region A	$\xi = \rho/h_r$,	$\eta = 2\theta/\pi$	(solid)
Region B	$\xi = (\rho - h_r)/(h - h_r) + 1$,	$\eta = 2\theta/\pi$	(solid)
Region C	$\xi = (\rho - h)/(L - h) + 2$,	$\eta = 2\theta/\pi$	(melt)
Mapping II			
Region E	$\xi = r$, $\eta = zL/2h$		(solid)
Region F	$\xi = r$, $\eta = [1 - (1/2)(L - z)/(L - h)]L$		(melt)

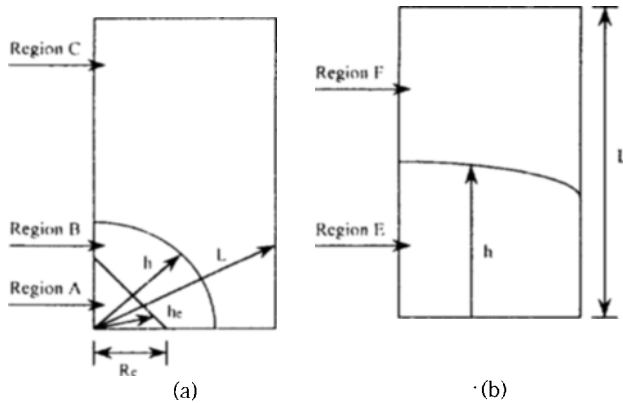


Fig. 2. Schematics of two mapping rule and used symbols (a) Mapping I and (b) Mapping II.

linearities caused by the unknown shape of the melt/crystal interface.

Using only one mapping rule used in the previous works cannot simulate the transition from hemispherical to planar interface, so that two mapping rule method should be used. The relationship between the transformed and the original coordinate system is shown in Table 2. The mapping I and the mapping II techniques use radial and rectangular Cartesian coordinate system, respectively. The mapping I and the mapping II are used for the computation of the hemispherical and the planar melt/crystal interface. In region A at the mapping I, h_r is used for imposing the essential boundary condition at the heat exchanger. The symbols and the mapping regions used in Table 2 are shown in Fig. 2.

2. Finite Element Formulation

The temperature field $T(r, z, t)$ and the interface location $h(r, z, t)$ are represented in expansions of finite element basis functions and unknown coefficients, such as,

$$T(r, z, t) = T(\xi, \eta, t) = \sum_{i=1}^N \alpha_i(t) \Phi^i(\xi, \eta) \tag{9}$$

$$h(r, z, t) = \begin{cases} h(\eta, t) = \sum_{i=1}^M \beta_i(t) \Psi^i(\eta) & (t \leq t_c) \\ h(\xi, t) = \sum_{i=1}^M \beta_i(t) \Psi^i(\xi) & (t \geq t_c) \end{cases} \tag{10}$$

where N and M are the numbers of basis functions associated with unknown coefficients in each expansion. Lagrangian bi-quadratic $\{\Phi\}$ and quadratic $\{\Psi\}$ finite element basis functions are used for representing temperature and melt/crystal interface shape, respectively. In Eq. (10), t_c is the time for chang-

ing the interface shape. The coefficient $\alpha_i(t)$, $\beta_i(t)$ are determined by the solutions of residual equations. The energy equation [Eq. (1)] and the boundary conditions [Eqs. (4)-(8)] are combined to form a set of Galerkin weighted residual equations. The weak form of the conservation equation is formed by summing these equations.

$$R_{r,j}^{(k)} = \int_D \left\{ \Phi^j \frac{dT(r, z, t)}{dt} + \alpha [\nabla_k \Phi^j \cdot \nabla_k T(\xi, \eta, t)] \right\} g_k d\xi d\eta + \int_{\partial D} \Psi^j Bi(T - T_\infty) dl, \quad j = 1, \dots, N. \tag{11}$$

where g_k is the determinants of the matrix tensors associated with coordinate transformations [Aris, 1962]. Subscript k is used to denote the different mapping region. The total time derivative in the weak form of conservation equations is shown due to the fixed interface location in the transformed coordinate system. The motion of the interface location in the original coordinate system can be considered as followed.

$$\frac{dT(r, z, t)}{dt} = \frac{\partial T(\xi, \eta, t)}{\partial t} + \frac{\partial T(\xi, \eta, t)}{\partial \xi} \frac{\partial \xi}{\partial t} + \frac{\partial T(\xi, \eta, t)}{\partial \eta} \frac{\partial \eta}{\partial t} \tag{12}$$

In the mapping rule, the fixed coordinate system (ξ, η) is related with time. For example, at the solid region in the mapping II

$$\frac{\partial \eta}{\partial t} = - \frac{zL}{2h^2} \frac{\partial h}{\partial t} \tag{13}$$

The thermal equilibrium condition [Eq. (2)] is converted to Galerkin weighted residual equations using the one-dimensional Lagrangian basis function defined on the melt/crystal interface.

$$R_{l,j} = \int_{\partial D} \Psi^j (T - T_m) dl, \quad j = 1, \dots, M. \tag{14}$$

3. Time-Integration Methods

For time-dependent calculations, implicit Euler method is used because no time derivatives appear in the residual equations formed from the thermal equilibrium condition. This singularity prevents the use of traditional explicit time integration methods [Ungar et al., 1988; Finlayson, 1980].

When the transition of the interface shape is occurred from hemispherical to planar, the temperature field in the transformed coordinate using mapping II is approximated with it using mapping I through the temperature field in the original coordinate system. The interface location at this time is also approximated. The interface location $h(R, 0, t_c)$ at the mapping II cannot be defined exactly, so very small number ϵ is used and the values of ϵ is 10^{-13} .

NUMERICAL ANALYSIS

The efficiency and the accuracy of this numerical method were studied by comparing the results from proposed numerical method with the results from only temperature field. Newton iteration are continued until the largest change in any component of the correction vector is less than 10^{-8} . The model problem was not linear when viewed as a moving boundary problem, so multiple iterations were necessary for each

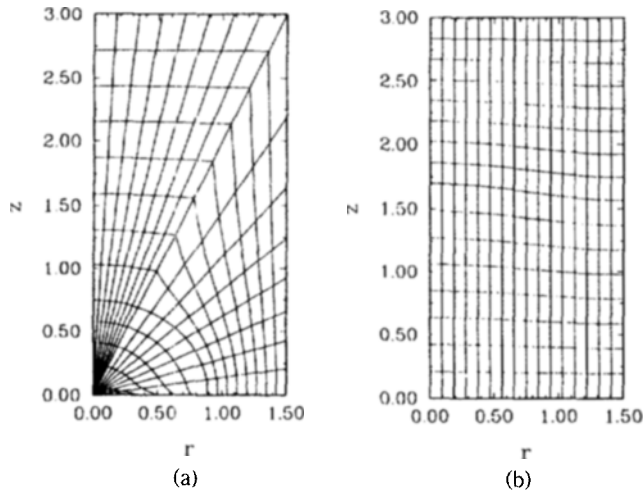


Fig. 3. Typical finite element meshes projected into the original coordinate system (a) Mapping I and (b) Mapping II.

time step to converge to the solution. Several iterations are needed and quadratic convergence is attained.

A typical finite element meshes mapped back to the original coordinate system are shown in Fig. 3. To compare the solutions of moving boundary problem with single phase solution, the thermal energy (E) is defined in the original coordinate system.

$$E = \int_D \frac{T \cdot T}{2} dA \quad (15)$$

In this case, the heat exchanger temperature T_o is -250°C and the excess heating temperature is 100°C . The dimensional Biot number Bi is zero, the height of crucible H is 3.0 cm and the cooling zone radius R_c is 0.375 cm. The comparison of the thermal energy and the maximum temperature (T_{max}) in the whole calculation domain was shown together in Fig. 4.

The temperature field and the location of moving boundary at several time step are shown in Fig. 5 for this case. As shown in Fig. 5, the hemispherical interface shape of solid/melt BGO becomes planar.

To investigate the curvature of interface, the deflection of the melt/crystal interface Δ at each time step is defined as

$$\Delta \equiv \max_i (h_z)_i - \min_i (h_z)_i, \quad i = 1, \dots, M. \quad (16)$$

where h_i is the distance for z -direction of the interface location shape function h . The deflection of melt/crystal interface is shown in Fig. 6. The maximum deflection Δ_{max} is shown at time t_i when the interface shape changes from hemispherical to planar.

RESULTS AND DISCUSSION

Calculations were performed using the growth parameter values in Table 1. The effects of the growth parameters on the interface shape and the temperature field were investigated. In standard case, the heat exchanger temperature T_o is -250°C and the excess heating temperature is 100°C . The dimensional Biot number Bi is zero cm^{-1} , the height of crucible H is 3.0 cm and the ratio of the crucible radius to the cooling zone radius

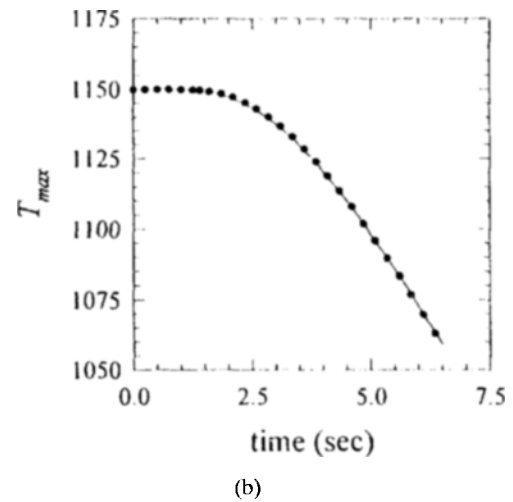
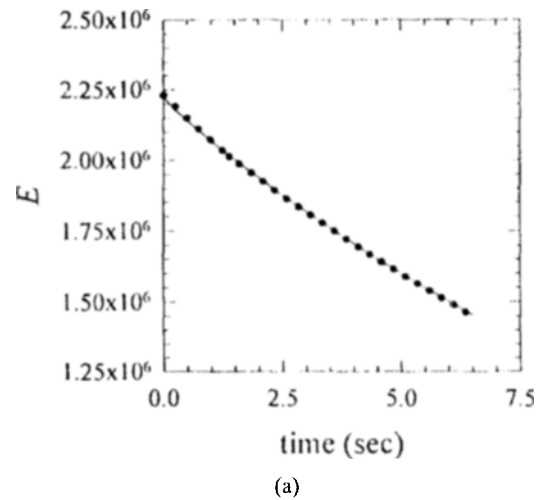


Fig. 4. Comparison of (a) the thermal energy and (b) the maximum temperature in the whole calculation domain. The solid line and the dotted line are the results of the model without and with the moving boundaries, respectively.

R/R_c is 7.

1. Effects of the Excess Heating Temperature

The excess heating temperature ΔT is one of the important growth parameters which affect the deflection of the melt/solid interface. It was varied from 25 to 150°C , while values of other growth parameters were set for the standard case. As the excess heating temperature was increased, t_i increased but Δ_{max} decreased as shown in Fig. 7. As it is increased, more growth time for whole process is required but the quality of BGO crystal may be improved.

2. Effects of the Heat Exchanger Temperature

The heat exchanger temperature T_o can be controlled by the flow rate of helium gas through the heat exchanger. It is also the important growth parameter. To investigate the effects of heat exchanger temperature, it has been changed from -250 to 750°C . In this case, other growth conditions were fixed at the standard process. As the heat exchanger temperature was increased, t_i increased but Δ_{max} decreased as shown in Fig. 8.

3. Effects of the Crucible Geometry

The ratio of the height to the radius of the crucible H/R has

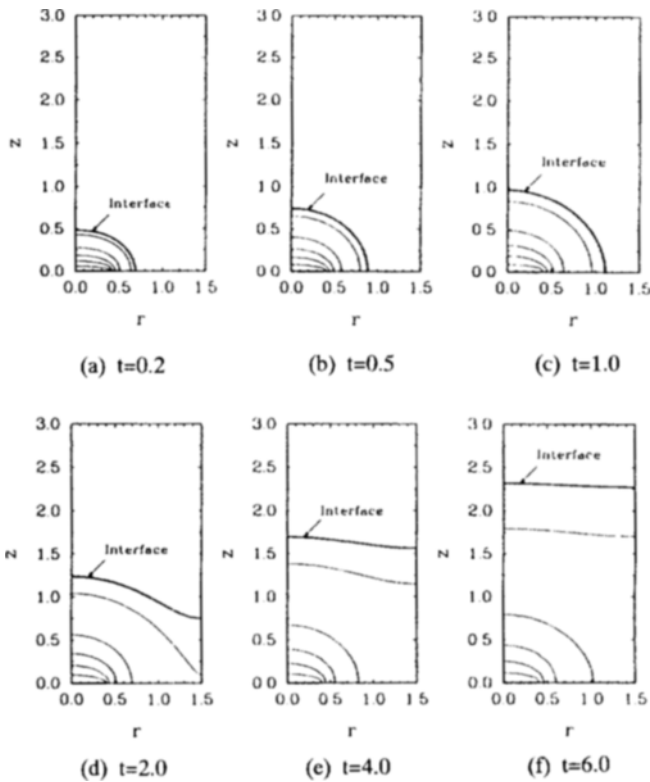


Fig. 5. Transient temperature fields for the HEM growth of BGO crystal with the moving boundary (The difference between isotherms is 250°C).

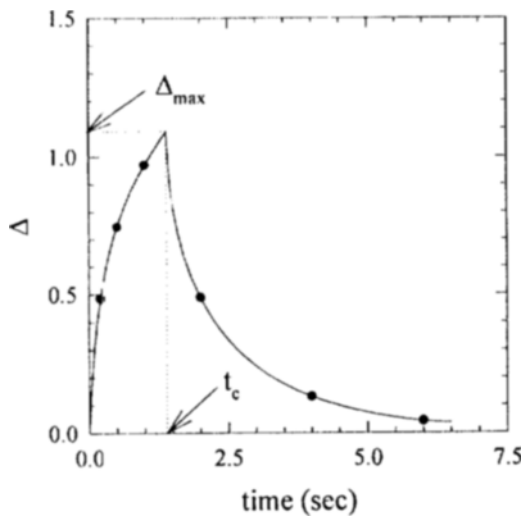


Fig. 6. The deflection of melt/solid interface predicted by two mapping method. The six points denote the time step shown in previous figure.

been varied to examine the effect on the interface deflection. It was varied from 1.0 to 3.0, for which the result is shown in Fig. 9. As the ratio was increased, t_c and Δ_{max} kept almost constant except for 1.0 case. The aspect ratio hardly affects the deflection of BGO melt/solid interface when it is greater than 1.5.

4. Effects of the Cooling Zone Radius

The effects of cooling zone radius R_c were studied by chang-

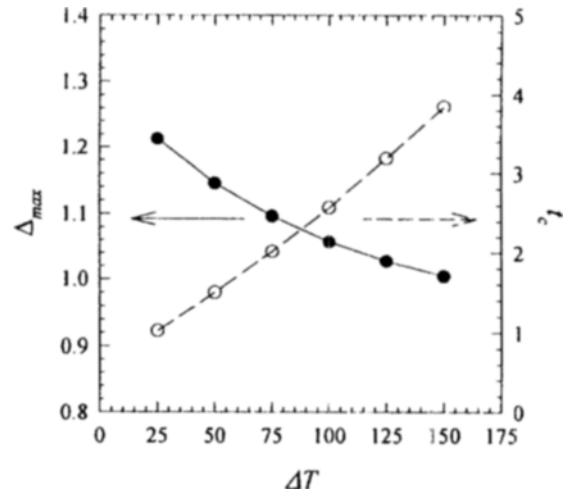


Fig. 7. The effects of ΔT on Δ_{max} and t_c .

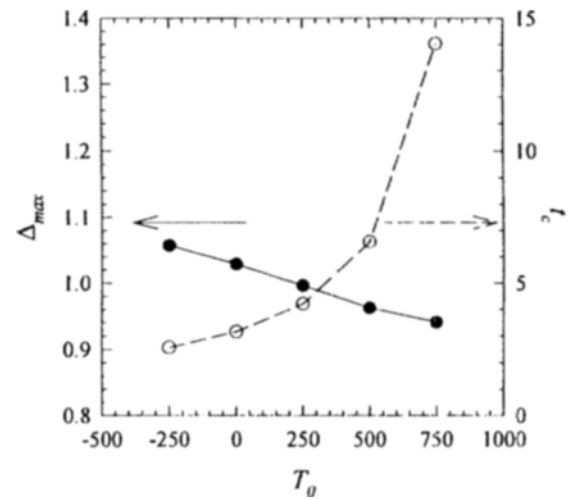


Fig. 8. The effects of T_0 on Δ_{max} and t_c .

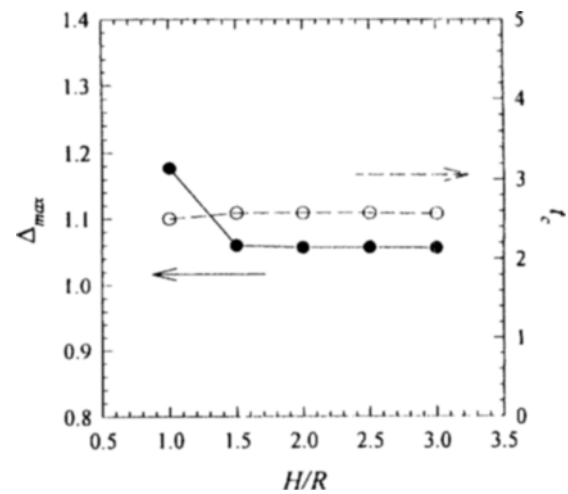


Fig. 9. The effects of H/R on Δ_{max} and t_c .

ing the ratio of the crucible radius to the cooling zone radius R/R_c from 4.0 to 10.0. As it is increased, the cooling zone radius

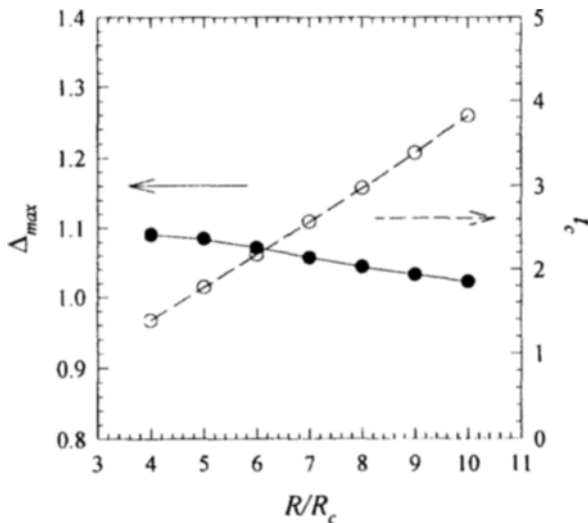


Fig. 10. The effects of R/R_c on Δ_{max} and t_c .

is decreased. As R/R_c was increased, t_c increased and Δ_{max} decreased as shown in Fig. 10.

5. Effects of the Heat Transfer between the Crucible and the Heating Element

To investigate the conductive and convective heat transfer between the crucible and the heating element, the dimensional Biot number Bi was changed from 0 to 0.1 cm^{-1} . As it is increased, the heat transfer between the crucible and the heating element is increased. As the heat transfer was increased, the deflection at the latter time step increased suddenly as shown in Fig. 11. From these result the heat transfer between the crucible and the heating element should be suppressed to maximize the planarity of the interface shape.

CONCLUSION

The HEM model for growth of BGO crystal has been developed to simulate the heat transfer process. The moving boundary problems for the temperature field and the melt/solid interface location were solved using the two mapping rule method which is a modification of the finite element isotherm-Newton method. The finite element methods described here are rigorous and effective to solve the moving boundary problems with the transition of the interface shape from hemispherical to planar. With this numerical method, the interface location at each time step was obtained as a part of solution and the curvature of the interface could be investigated.

The effects of the various growth parameters were examined on the interface shape and the temperature profile using this model. The maximum deflection is shown at the time for changing the interface shape. As the excess heating temperature was increased, more growth time for whole process is required but the quality of BGO crystal may be improved. As the heat exchanger temperature was increased, t_c increased but Δ_{max} decreased. The ratio of the height to the radius of crucible hardly affects the deflection of BGO melt/solid interface when it is greater than 1.5. As the cooling zone radius is decreased, Δ_{max} is decreased. The heat transfer between the crucible and the heat

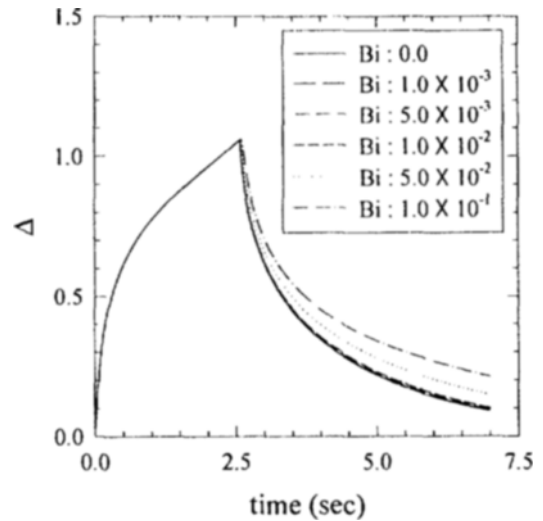


Fig. 11. The effects of Bi on Δ .

ing element should be suppressed to maximize the planarity of the interface shape.

NOMENCLATURE

Bi	: dimensional Biot number [cm^{-1}]
E	: thermal energy defined in Eq. (15)
h	: interface shape function [cm]
h_e	: pseudo interface shape function for imposing the essential boundary conditions [cm]
h_z	: distance in z direction of interface shape function [cm]
H	: height of crucible [cm]
M	: number of basis functions associated with interface location
N	: number of basis functions associated with temperature
r	: radial coordinate [cm]
R	: radius of crucible [cm]
R_c	: radius of cooling zone [cm]
R_{T_i}	: residual equation for temperature
R_{L_i}	: residual equation for interface location
t	: time [sec]
t_c	: time for change the melt/solid interface shape [sec]
T	: temperature [$^{\circ}\text{C}$]
T_m	: melting temperature of BGO [$^{\circ}\text{C}$]
T_w	: temperature of heating element [$^{\circ}\text{C}$]
T_o	: temperature of heat exchanger [$^{\circ}\text{C}$]
z	: axial coordinate [cm]

Greek Letters

α	: thermal diffusivity of BGO [cm^2/sec]
α_i	: unknown coefficient associated with temperature
β_i	: unknown coefficient associated with interface location
Δ	: deflection of melt/solid interface defined in Eq. (16)
Δ_{max}	: maximum interface deflection
ΔT	: excess heating temperature [$^{\circ}\text{C}$]
ϵ	: small number
ξ	: imaginary coordinate
η	: imaginary coordinate
ρ	: cylindrical coordinate [cm]

- θ : cylindrical coordinate [rad]
 Φ : Lagrangian biquadratic finite element basis function
 Ψ : Lagrangian quadratic finite element basis function

REFERENCES

- Aris, R., "Vectors, Tensors and the Basic Equations of Fluid Mechanics", Prentice-Hall, Englewood Cliffs, 1962.
- Berkowski, M., Iliev, K., Nikolov, V., Peshev, P. and Piekarczyk, W., "Conditions of Maintenance of a Flat Crystal/Melt Interface during Czochralski Growth of Bismuth Germanium Oxide Single Crystals", *J. Crystal Growth*, **108**, 225 (1991).
- Bird, R. B., Stewart, W. E. and Lightfoot, E. N., "Transport Phenomena", John Wiley & Sons, New York, 1960.
- Ettouney, H. M. and Brown, R. A., "Finite-Element Methods for Steady Solidification Problems", *Comput. Phys.*, **49**, 118 (1983).
- Fan, S., Shan, G., Li, J. and Wang, W., "Industrial Bridgman Growth of Large Size BGO Crystal with Special Shapes", *Crystal Properties and Preparation*, **36-38**, 42 (1991).
- Finlayson, B. A., "Nonlinear Analysis in Chemical Engineering", McGraw-Hill, New York, 1980.
- Gallagher, R. H., Oden, J. T., Zienkiewicz, O. C., Kawai, T. and Kawahara, M., "Finite Elements in Fluids", John Wiley & Sons, New York, 5, 1984.
- Gelinas, R. J., Doss, S. K. and Miller, K., "The Moving Finite Element Method: Applications to General Partial Differential Equations with Multiple Large Gradients", *J. Comput. Phys.*, **40**, 202 (1981).
- Hood, P., "Frontal Solution Program for Unsymmetric Matrices", *Int. J. Num. Meth. Eng.*, **10**, 379 (1976).
- Kaldis, E., "Crystal Growth of Electronic Materials", Elsevier Science Publishers B. V., 1985.
- Kawano, K., Yoshida, T., Nakata, R., Yamada, N. and Sumita, M., "Crystal Growth of $\text{Bi}_4\text{Ge}_3\text{O}_{12}$ and Heat Transfer Analyses of Horizontal Bridgman Techniques", *Jpn. J. Appl. Phys.*, **32**, 1736 (1993).
- Lynch, D. R. and Gray, W. G., "Finite Element Simulation of Flow in Deforming Regions", *J. Comput. Phys.*, **36**, 135 (1980).
- Quon, D. H. H., Chehab, S., Aota, J., Kuriakose, A. K., Wang, S. S. B., Saghir, M. Z. and Chen, H. L., "Float-Zone Crystal Growth of Bismuth Germanate and Numerical Simulation", *J. Crystal Growth*, **134**, 266 (1993).
- Saito, H. and Scriven, L. E., "Study of Coating Flow by the Finite Element Method", *J. Comput. Phys.*, **42**, 53 (1981).
- Schmid, F., Khattak, C. P. and Felt, D. M., "Producing Large Sapphire for Optical Applications", *Am. Ceram. Soc. Bull.*, **73**, 39 (1994).
- Shigematsu, K., Anzai, Y., Omote, K. and Kimura, S., "Thermal Properties of Molten Bismuth Germanates", *J. Crystal Growth*, **137**, 509 (1994).
- Takagi, K. and Fukazawa, T., "Effect of Growth Conditions on the Shape of $\text{Bi}_4\text{Ge}_3\text{O}_{12}$ Single Crystals and on Melt Flow Patterns", *J. Crystal Growth*, **76**, 328 (1986).
- Ungar, L. H., Ramprasad, N. and Brown, R. A., "Finite Element Methods for Unsteady Solidification Problems Arising in Prediction of Morphological Structure", *J. Sci. Comput.*, **3**, 77 (1988).
- Weber, M. J. and Monchamp, R. R., "Luminescence of $\text{Bi}_4\text{Ge}_3\text{O}_{12}$: Spectral and Decay Properties", *J. Appl. Phys.*, **44**, 5495 (1973).